Mutations in *KAT6B*, Encoding a Histone Acetyltransferase, Cause Genitopatellar Syndrome

Philippe M. Campeau,[1,17] Jaeseung C. Kim,[2,17] James T. Lu,[3,4] Jeremy A. Schwartzentruber,[5] Omar A. Abdul-Rahman,[6] Silke Schlaubitz,[1] David M. Murdock,[3] Ming-Ming Jiang,[1] Edward J. Lammer,[7] Gregory M. Enns,[8] William J. Rhead,[9] Jon Rowland,[10] Stephen P. Robertson,[11] Valérie Cormier-Daire,[12] Matthew N. Bainbridge,[3,4] Xiang-Jiao Yang,[13,14] Marie-Claude Gingras,[1,3] Richard A. Gibbs,[1,3] David S. Rosenblatt,[2,14,15] Jacek Majewski,[2,5] and Brendan H. Lee[1,16,*]

Genitopatellar syndrome (GPS) is a skeletal dysplasia with cerebral and genital anomalies for which the molecular basis has not yet been determined. By exome sequencing, we found de novo heterozygous truncating mutations in *KAT6B (*lysine acetyltransferase 6B, formerly known as *MYST4* and *MORF*) in three subjects; then by Sanger sequencing of *KAT6B*, we found similar mutations in three additional subjects. The mutant transcripts do not undergo nonsense-mediated decay in cells from subjects with GPS. In addition, human pathological analyses and mouse expression studies point to systemic roles of KAT6B in controlling organismal growth and development. *Myst4* (the mouse orthologous gene) is expressed in mouse tissues corresponding to those affected by GPS. Phenotypic differences and similarities between GPS, the Say-Barber-Biesecker variant of Ohdo syndrome (caused by different mutations of *KAT6B*), and Rubinstein-Taybi syndrome (caused by mutations in other histone acetyltransferases) are discussed. Together, the data support an epigenetic dysregulation of the limb, brain, and genital developmental programs.

Genitopatellar syndrome (GPS) [MIM 606170] is a rare skeletal dysplasia combining hypoplastic or absent patellae, genital anomalies, craniofacial defects, and intellectual disability among other features. It has been described in 18 subjects to date.[1–11] In one patient, we discovered a microdeletion encompassing *LMX1B* (explaining the patellar anomalies) and *NR5A1* (explaining the genital anomalies) though this was not found to be a recurrent molecular lesion in the other subjects.[11] An important phenotypic difference is that the subject with the microdeletion is not microcephalic although all other subjects are.

To gain insights into the molecular cause of GPS, we recruited subjects with this disease (see Figure 1 for photos, Figure S1 [available online] for pedigrees, and Table 1 and references therein for clinical details). Families provided informed consent to our study approved by the institutional review board of the Baylor College of Medicine. Subject 3 died at 8 years of age from bowel malrotation that led to volvulus and intestinal necrosis. An autopsy showed dramatic pancreatic hyperplasia (103 g for an expected weight of 15 g) with hyperplasia of some of the islets of Langerhans. An enlarged pancreas has never been described in other subjects, even though all other subjects in this study had abdominal ultrasounds. Other significant findings included kidney hypoplasia with multiple small subcapsullar cysts, a prominent suprapubic fat pad with underdeveloped clitoris and labia minora, and an anteriorly placed anus. Skeletal features included flat temporal bones, brachydactyly, flexion deformities of the hips and knees, and markedly hypoplastic patellae. Neuropathology showed microcephaly (851 g for an expected weight of 1,273 g); mild to moderate diffuse cortical atrophy; hypoplasia of the anterior portion of the corpus callosum; generalized mild gliosis; and small perivascular psammomatous calcifications in the basal ganglia, thalamus, corpus callosum, choroid plexus, and periventricular regions. See Figures 2A–2D for histology of some relevant tissues. Psammoma bodies are calcifications frequently seen in meningiomas and other malignancies (and only rarely in benign overgrowths) and are thought to result from calcification of dead cells or an active process to inhibit cell growth.[12]

We performed whole-exome sequencing on three subjects (subjects 2, 4, and 5). For subjects 2 and 4, exomes were captured on Nimblegen's SeqCap EZ V2.0

[1]Department of Molecular and Human Genetics, Baylor College of Medicine, Houston, TX 77030, USA; [2]Department of Human Genetics, McGill University, Montreal, QC H3A 1B1, Canada; [3]Human Genome Sequencing Center, Baylor College of Medicine, Houston, TX 77030, USA; [4]Department of Structural and Computational Biology and Molecular Biophysics, Baylor College of Medicine, Houston, TX 77030, USA; [5]McGill University and Genome Quebec Innovation Centre, Montreal, QC H3A 1A4, Canada; [6]Division of Medical Genetics, Department of Pediatrics, University of Mississippi Medical Center, Jackson, MS 39216, USA; [7]Division of Medical Genetics, Children's Hospital and Research Center, Oakland, CA 94609, USA; [8]Division of Medical Genetics, Department of Pediatrics, Stanford University, Stanford, CA 94305, USA; [9]Department of Pediatrics, Section of Genetics, Medical College of Wisconsin, Milwaukee, WI 53226, USA; [10]Pathology and Clinical Lab Medicine, Children's Hospital and Research Center, Oakland, CA 94609, USA; [11]Department of Pediatrics, Dunedin School of Medicine, Dunedin 9054, New Zealand; [12]Département de Génétique, Unité Institut National de la Santé et de la Recherche Médicale (INSERM) U781, Université Paris Descartes, Sorbonne Paris Cité, Hôpital Necker Enfants Malades, 15 Paris Cedex, France; [13]Goodman Cancer Center, McGill University, Montreal, QC H3A 1A3, Canada; [14]Department of Medicine, McGill University Health Center, Montreal, QC H3A 1A1, Canada; [15]Departments of Pediatrics and Biology, McGill University, Montreal, QC H3A 2T5, Canada; [16]Howard Hughes Medical Institute, Houston, TX 77030, USA
[17]These authors contributed equally to this work
*Correspondence: blee@bcm.edu
DOI 10.1016/j.ajhg.2011.11.023.

Figure 1. Clinical Presentation of Subjects with GPS
Photographs of (A) subject 2 at 9 years of age, (B) subject 3 at 8 years of age, and (C) subject 5 at birth and at 8 months of age.

library and sequencing was conducted on Illumina HiSeq. Sequences were aligned to the human reference genome (hg18) with Burrows-Wheeler Aligner (BWA) (v 0.5.9)[13] and recalibrated with the Genome Analysis Toolkit (GATK). Both samples achieved over 91% targeted bases at 20× coverage. SNPs and insertion-deletion events were called with Samtools Pileup (version 0.1.17).[14] Variants were annotated with ANNOVAR[15] and protein-impacting variants that were rare (minor allele frequency $< 5\%$), novel, and nonsynonymous were preferentially explored. We narrowed gene candidates by comparing with known functional databases such as dbNSFP[16] and SWISS-PROT[17] to narrow down the list of plausible causative variants. For subject 5, the exome was captured on the Agilent SureSelect 50 Mb oligonucleotide library. DNA was sheared by sonication to an approximately 200 bp length. Fragment ends were ligated to specific adaptors and capture was performed with the manufacturer's protocol. The captured exome was reamplified by PCR (12 cycles) then applied to a single lane of Illumina HiSeq sequencer. The Illumina reads were aligned to the reference human genome (hg19) with BWA (v. 0.5.9) and Samtools (v. 0.1.12a). Pileup and varFilter commands were used to call variants, and these were filtered to retain SNPs and insertion-deletions with Phred-like quality scores of at least 20 and 50, respectively. ANNOVAR was used to annotate nonsynonymous variants according to the type of mutation, occurrence in dbSNP, SIFT score,[18] and 1000 Genomes allele frequency.[19]

As shown in Table 2, only 13 genes showed rare novel variants that were potentially pathogenic and were shared by the three subjects. Variants were visualized and compared to the exomes of 20 other subjects with unrelated conditions. When keeping only high-quality variants (e.g., removing probable false positive variants in repeat regions or variants seen in unrelated conditions), only *KAT6B* variants remained. All variants were frameshift insertions-deletions (Figure 3, Figures S2A–2C, available online, and Table 3; RefSeq NM_012330.2 was used for the positions). We confirmed the variants by Sanger sequencing and sequenced the complete coding sequence of the gene in the other individuals recruited in our study (see Table S1 for primers). We have thus identified nonsense mutations in two additional subjects and one of the previously identified frameshift deletions in another (Figure 3 and Figures S2D–2F). Analysis of parental samples from five subjects showed that the mutations were acquired de novo (Figure S2). All mutations lead to a loss of the highly conserved transcription activation domain (Figure 3 and Figure S3). The Exome Variant Server has public information on *KAT6B* for over 1,100 individuals of European descent and 900 African Americans, with an average coverage of over 85× for the coding sequences of *KAT6B*. No truncating mutations of *KAT6B* were identified in this server or in other exomes performed by Baylor College of Medicine's Human Genome Sequencing Center.

Lymphoblastoid cells were established by Epstein-Barr virus infection for subjects 1 through 4. One million cells were collected, and RNA was extracted with Trizol, treated with DNase I, then phenol-chloroform extracted. The first strand of cDNA was synthesized with oligo dT primers via Invitrogen's SuperScript III First-Strand synthesis kit. For RT-PCR, a 5′ nuclease assay from Integrated DNA Technologies (Coralville, IA) was designed with probes having a 5′ fluorescein amidite fluorophore, a 3′ IBFQ quencher, and an internal ZEN quencher (see Table S1). Quantitative real-time PCR was performed in an ABI 7900 HT machine with ABI's TaqMan Universal PCR Master Mix according to the manufacturer's instructions (Figure 4A). We also amplified cDNA by using primers encompassing the last exon-exon junction and the most 5′ mutations and sequenced the products (see Table S1 for primers). These experiments demonstrate that the mutant mRNAs do not undergo nonsense-mediated decay (Figures 4A and 4B), which is consistent with localization of the premature stop codons in the last exon. To assess the expression pattern of *Myst4* in organs known to be affected by GPS, we performed immunohistochemistry on mice of various developmental ages. The primary antibody used is Sigma AV38985 (1:200 dilution), the secondary is Invitrogen A-11012 (1:600 dilution). The specificity of the antibody for the mouse protein was confirmed by showing a staining pattern in the brain compatible with published RNA in situ experiments[20] (see Figure 5A). *Myst4* is strongly expressed in the telencephalic vesicles, trigeminal ganglion, spinal cord, dorsal root ganglia, digestive

Table 1. Clinical Features of Enrolled Subjects and 13 Other Subjects from the Literature

Subjects	1	2	3	4	5	6	Literature[a]	Total (Affected/Total)
Gender	female	male	female	male	female	male	4 females/9 males	7 females/12 males
Skeletal[b]								
Absent or hypoplastic patellae	+	+	+	+	+	+	12	18/19
Flexion deformities	+	+	+	+	+	+	13	19/19
Club feet	+	+	+	+	+	+	12	18/19
Thoracolumbar kyphosis or scoliosis				+	+		3	5/19
Pelvic anomalies	+			+			5	7/19
Costal anomalies	+		+	+			1	4/19
Neurological[c]								
Microcephaly	+	+	+	+	+	+	13	19/19
Developmental delay or intellectual disability	+	+	+	+	+	+	10/10[d]	16/16
Absent or thin corpus callosum	+	+	+	+	+	+	9	15/19
Colpocephaly or ventriculomegaly	+			+	+		1	4/19
Pachygyria						+	2	3/19
Subependymal periventricular nodular heterotopia						+	1	2/19
Optic atrophy or cortical visual impairment		+	+	+			0	3/19
Hearing loss	+	+					1	3/19
Anal and Genital[e]								
Anteriorly positioned anus	+		+				1	3/19
Anal atresia or stenosis				+		+	0	2/19
Hypoplastic labia minora or majora	+		+		+		3	6/6
Clitoromegaly	+				+		3	5/6
Scrotal hypoplasia		+		+		+	9	12/12
Cryptochidism		+		+		+	9	12/12
Renal[f]								
Hydronephrosis	+	+		+	+		11	16/19
Multicystic kidneys			+			+	4	6/19
Cardiac[g]								
Atrial septal defect	+		+	+		+	3	7/19
Ventricular septal defect				+			3	4/19
Facial[h]								
Facial dysmorphisms	+	+	+	+	+	+	13	19/19
Broad nasal bridge	+	+					7	9/19
Prominent nasal bridge			+	+			3	5/19

Table 1. *Continued*

Subjects	1	2	3	4	5	6	Literature[a]	Total (Affected/Total)
Other[i]								
Tracheo or laryngomalacia		+	+				4	6/19
Feeding difficulties		+	+	+	+		2	6/19
Small bowel malrotation			+				1	2/19
Hypothyroidism					+		2	3/19

[a] From Armstrong and Clarke,[2] Bergmann et al.,[3] Brugha et al.,[4] Cormier-Daire et al.,[5] Goldblatt et al.,[6] Penttinen et al.,[9] and Reardon[10].
[b] Occasional findings include osteoporosis, radioulnar synostosis, radial head deformity, brachydactyly, short stature, joint laxity, dislocated patellae, undertubulation of long bones, coxa vara, camptodactyly, narrow thorax, and exostoses.
[c] Occasional findings include hypotonia, hypertonia, seizures, and subdural hemorrhage (subject 5).
[d] Ten out of thirteen children survived beyond neonatal period and were included.
[e] Occasional findings include rectal duplication (subject 6) and underdeveloped clitoris (subject 3).
[f] Occasional findings include fused renal ectopia, dysplastic kidneys, and hypoplastic kidneys (subject 3).
[g] Occasional findings include tortuous ascending aorta, dilated aortic arch, patent ductus arteriosus, patent foramen ovale, and stenosis of the pulmonary valve.
[h] Occasional findings include bulbous nose, retrognatia or micrognatia, cleft or high-arched palate, gingival hyperplasia, coarse facies, full cheeks, ear anomalies, dental anomalies, sparse hair, hypertelorism, plagiocephaly, bitemporal flattening, downslanting palpebral fissures, downturned corners of the mouth, short columella, short philtrum, tented upper lip, and midface hypoplasia.
[i] Occasional findings include hypogonadotrophic hypogonadism, respiratory distress, apnea, recurrent infections, single palmar crease, and skin laxity.

tract, pancreas liver and ribs of developing embryos (Figures 5A and 5B). After birth, it is strongly expressed in the diaphysis of the long bones, the kidney, and the patella, among other organs (Figures 5C–5K).

KAT6B has a highly conserved acetyltransferase domain[21] and has been shown to fuse with p300 and CBP following chromosomal translocations in acute myeloid leukemia and myelodysplastic syndrome.[22]

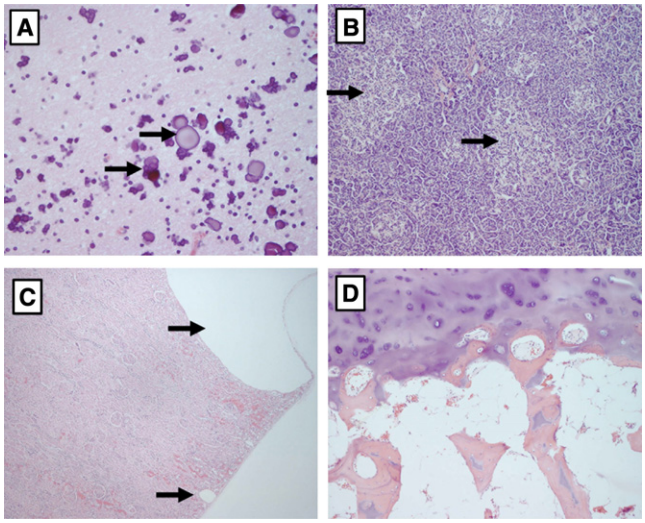

Figure 2. Hematoxylin and Eosin Images of Tissues from the Autopsy of Subject 3
Tissues shown are (A) the brain (400×) where we show a large cluster of perivascular calcifications in the white matter of the cerebral cortex (arrows point to two of them); these are never present in normal tissue; (B) the pancreas (100×) showing numerous islets of Langerhans, some of which are hyperplastic (black arrows), whereas others are of normal size (red arrows); (C) the kidney (100×), where we show one large and one small subcapsular cyst (arrows), and (D) the severely hypoplastic patella (100×), where there is persistence of the cartilaginous core of the trabeculae (black arrow).

KAT6B has been reported to interact with the RUNX family of transcription factors[22] and form a tetrameric complex with BRPFs, ING5, and EAF6.[23,24] KAT6B was pulled down in a PPAR-alpha interacting cofactor complex,[25] and a yeast two-hybrid screen identified Atrophin-1 as a binding partner of KAT6B.[26] Independently to its cloning in humans, the mouse ortholog of *KAT6B* was identified by screening a gene-trap library for genes highly expressed in the telencephalon.[20] Mice carrying a hypomorphic mutation of *Myst4* have short stature, an absence of fusion of the tibia and fibula, microcephaly with neurogenesis defects, early demise, and infertility.[27] A subject with a Noonan-like phenotype has recently been identified to harbor a chromosomal translocation disrupting *KAT6B* after exon 3, and the mRNA levels in lymphoblastoid cells were half of normal.[28] Given the phenotypic difference between the subject with a Noonan-like phenotype and subjects with

Table 2. Number of Variants Identified

	Subject 2	Subject 4	Subject 5	Shared (2 of 3)	Shared (3 of 3)
Total variants	2654026	2760221	490885		
Total variants after base quality filtering	1090174	1115186	256344		
Novel variants (dbSNP129/1000G)	872368	886839	237419		
Genes with rare nonsynonymous variants, splice site variants, insertions or deletions variants in coding regions.	440	367	273	76	13

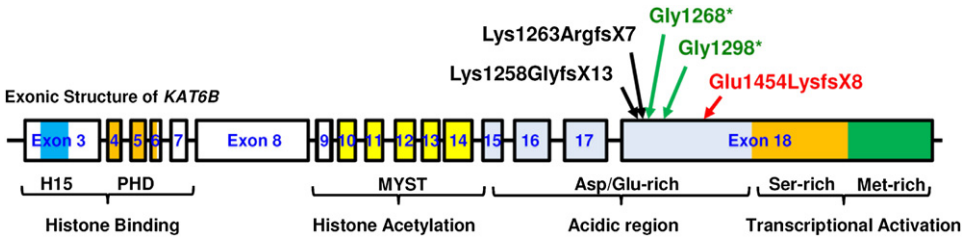

Figure 3. Location of Mutations Identified in KAT6B
The five different mutations form a cluster within the C-terminal acidic domain of KAT6B. The 16 coding exons and the corresponding introns of *KAT6B* are depicted with boxes and solid lines, respectively, with introns not shown to scale. The encoding domains are indicated below the exon-intron organization, along with the corresponding functions. The longest isoform is shown (isoform 1 in uniprot, a.k.a. MORF-beta, CCDS7345, 2073 aa). The following abbreviations are used: H15, histone H1- or H5-like domain; PHD, tandem plant homeodomain-linked zinc fingers. The amino acid changes resulting from five independent mutations present in 6 different subjects are indicated above the schematic exon-intronic structure. The mutations result in C-terminal truncation and remove the transcriptional activation domain, with the resulting mutant impaired in transcriptional activation. Deletions are shown in black arrows, nonsense mutations in green, and the complex insertion-deletion mutation in red. Sequence details of the mutations are shown in Table 3.

GPS (Table 4), the persistent expression of a truncated protein in GPS, containing intact N-terminal domain and HAT domains but lacking the C-terminal transcriptional activation domain, most likely leads to dominant-negative or gain-of-function effects on cellular signaling. Of relevance, leukemia-associated translocations also generate similar KAT6B fragments fused to p300 and CBP.[22] Rubinstein-Taybi syndrome [MIM 180849] is caused by de novo mutations inactivating the histone acetyltransferase activity of the latter two enzymes, and both haploinsufficiency and dominant-negative models have been postulated for this condition.[29,30] Although the presentation is distinct from GPS, the two conditions share some facial features, as well as intellectual disability, malformations of the heart and kidneys, and undescended testes. Recently, similar de novo truncating in *KAT6B* mutations were identified in subjects with the Say-Barber-Biesecker variant of Ohdo syndrome [MIM 249620], which overlaps with Genitopatellar syndrome in terms of facial features and congenital heart defects.[31,32] The mutations are however usually located more distally in the C terminus, specifically in the transcriptional activation domain, and there are several clinical differences: structural brain defects, skeletal defects, anal anomalies, genital anomalies and renal defects are more severe or frequent in GPS, whereas ocular, dental, palatal, and thyroid defects are more severe or frequent in the Say-Barber-Biesecker variant of Ohdo syndrome. A comparison of the phenotypes of GPS, the Say-Barber-Biesecker variant of Ohdo syndrome, the child with a translocation involving *KAT6B*, and Rubinstein-Taybi syndrome is shown in Table 4.

We have thus identified mutations in the epigenetic regulator KAT6B in several subjects with GPS. Because this acetyltransferase is a ubiquitous transcriptional coactivator, searching for more binding partners and studying its role in skeletogenesis and development in general might lead to important insights into epigenetic dysregulation in GPS and related diseases.

Supplemental Data

Supplemental Data include three figures and one table and can be found with this article online at http://www.cell.com/AJHG/.

Acknowledgments

We thank the families for participating in this study. We thank Alyssa Tran, Stephanie Dugan, and Andrea Kwan for help enrolling subjects; Kyu Sang Joeng, Yangjin Bae, Jianning Tao, and Terry Bertin for help and advice with the experiments; and

Table 3. Mutations Identified in the Subjects

Subject	Mutation (DNA)	Mutation (Protein)	Parents Tested	Reference
1	c.3892G>T	p.Gly1298*	not available	subject 1 in Abdul-Rahman et al.[1] See also Schlaubitz et al.[11]
2	c.4360_4368delinsAAAAACCAAAA	p.Glu1454LysfsX8	de novo	subject 2 in in Abdul-Rahman et al.[1] See also Schlaubitz et al.[11]
3	c.3802G>T	p.Gly1268*	de novo	Lammer and Abrams[7] Schlaubitz et al.[11]
4	c.3769_3772delTCTA	p.Lys1258GlyfsX13	de novo	Lifchez et al.[8]
5	c.3788_3789delAA	p.Lys1263ArgfsX7	de novo	this report
6	c.3769_3772delTCTA	p.Lys1258GlyfsX13	de novo	this report

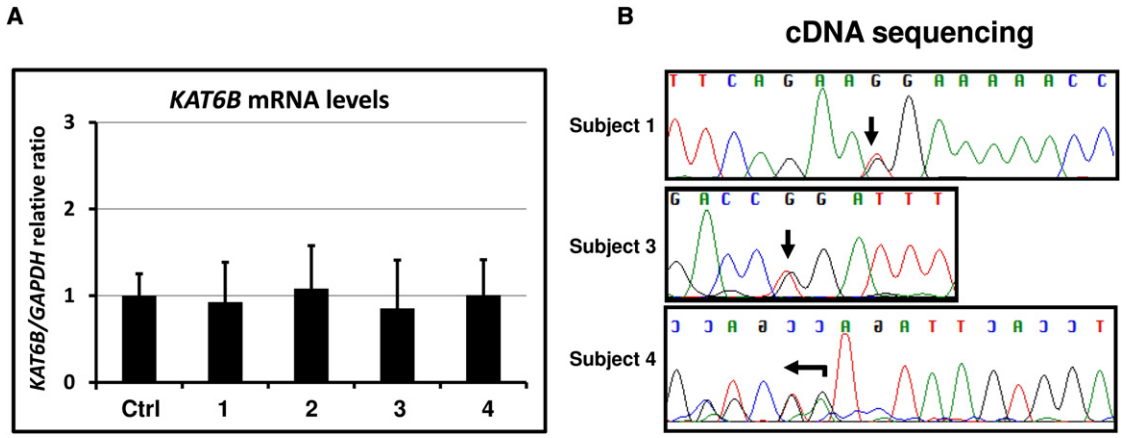

Figure 4. Mutant Transcripts Do Not Undergo Nonsense-Mediated Decay
(A) Messenger RNA levels of *KAT6B*, normalized to *GAPDH*, in lymphoblastoid cell lines derived from subjects 1–4, and from control cell lines (n = 3) (data are represented as mean ± standard error of the mean).
(B) Sequencing of cDNA from those cells to demonstrate definitively that the mutant transcripts do not undergo nonsense-mediated decay.

the University Center for Fetal Medicine of the University of Mississippi for help collecting clinical information. Philippe Campeau is funded in part by the Clinician-Scientist Training award of the Canadian Institutes of Health Research.

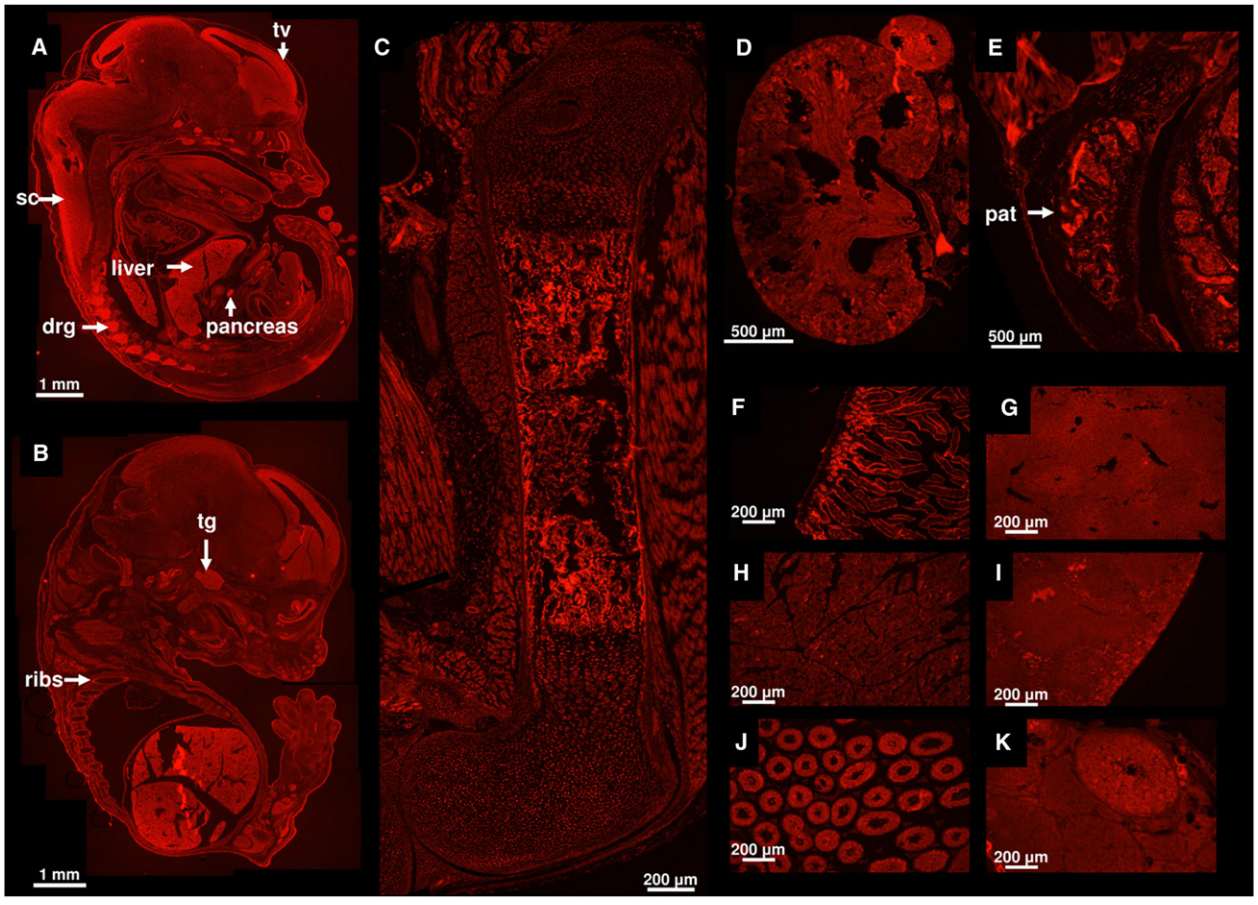

Figure 5. *Myst4* Expression in Wild-Type C57BL/6 Mice Detected by Immunohistochemistry
Tissues shown are (A) and (B) whole embryos at embryonic day 15.5, (C) femur at postnatal day 1, and (D) kidney at postnatal day 1. The other tissues are at 8 weeks of age: (E) patella, (F) duodenum (which required 2.5 s of exposure time instead of 5), (G) liver, (H) pancreas, (I) spleen, (J) testis, and (K) ovary. Arrows point to the telencephalic vesicles (tv), spinal cord (sc), liver, pancreas, dorsal root ganglia (drg), trigeminal ganglion (tg), ribs, and patella (pat).

Table 4. Phenotypic Differences between GPS, the Say-Barber-Biesecker Variant of Ohdo Syndrome, a Subject with a Translocation Truncating *KAT6B* after Exon 3, and Rubinstein-Taybi Syndrome

	Genitopatellar Syndrome	Say-Barber-Biesecker Variant of Ohdo Syndrome	Subject with Noonan-Like Phenotype and N-Terminal Truncation of KAT6B	Rubinstein Taybi Syndrome
Neurological anomalies	DD/ID,[a] microcephaly in all, agenesis of the corpus callosum, colpocephaly	DD/ID, microcephaly in minority, hypotonia, no structural defects	microcephaly, ADHD,[b] IQ 75-80, no structural defects	DD/ID, seizures, no structural defects
Facial anomalies	broad or prominent nasal bridge, bulbous nose in minority, full cheeks in minority	blepharophimosis, ptosis, broad and flat nasal bridge, bulbous nose, full cheeks, abnormal ears, small mouth, expressionless or mask-like facies	blepharophimosis, ptosis, arched eyebrows, abnormal ears, smooth philtrum, retrognatia, high-arched palate	arched eyebrows, downslanting palpebral fissures, beaked nose with the columella extending below the nares, high-arched palate, mild micrognathia, grimacing smile
Musculo-skeletal anomalies	absent or hypoplastic patellae in majority, flexion contractures, club feet, costo-vertebral anomalies, pelvic anomalies	long thumbs and toes, patellar anomalies in minority	short stature, retarded bone age, ligamentous laxity	short stature, joint hypermobility, broad thumbs and broad big toes
Anal and genital anomalies	anal anomalies, hypoplastic labia, clitoromegaly, scrotal hypoplasia, cryptorchidism	cryptorchydism and hypospadias		
Heart anomalies	congenital heart defects	congenital heart defects		congenital heart defects
Structural eye defects	none	frequent		frequent
Dental anomalies	rare	frequent		
Cleft palate	rare	frequent		
Hearing impairment	rare	frequent		
Thyroid abnormalities	rare	frequent		
Renal anomalies	hydronephrosis or cysts in a majority	vesicoureteric reflux in one individual		
Other	feeding difficulties, tracheomalacia, respiratory difficulties, small bowel malrotation	feeding difficulties		feeding difficulties, respiratory difficulties, skin anomalies (hirsutism, naevus flammeus on the forehead, and keloid formation), malignancies

[a] DD/ID is used as an abbreviation for developmental delay or intellectual disability.
[b] ADHD is used as an abbreviation for Attention deficit hyperactivity disorder.

Received: September 27, 2011
Revised: November 14, 2011
Accepted: November 22, 2011
Published online: January 19, 2012

Web Resources

The URLs for data presented herein are as follows:

1000 Genomes, http://www.1000genomes.org/
ANNOVAR, http://www.openbioinformatics.org/annovar/
BWA, http://bio-bwa.sourceforge.net/
dbNSFP, https://sites.google.com/site/jpopgen/dbNSFP
dbSNP, http://www.ncbi.nlm.nih.gov/projects/SNP/
Exome Variant Server, http://evs.gs.washington.edu/EVS/
GATK, http://www.broadinstitute.org/gsa/wiki/index.php/The_Genome_Analysis_Toolkit
Online Mendelian Inheritance in Man (OMIM), http://www.omim.org
Polyphen-2, http://genetics.bwh.harvard.edu/pph2/
Samtools Pileup, http://samtools.sourceforge.net/
Swiss-Prot, http://web.expasy.org/docs/swiss-prot_guideline.html
SIFT, http://sift.jcvi.org/
UCSC Genome Browser (hg18 and hg19), http://genome.ucsc.edu/

References

1. Abdul-Rahman, O.A., La, T.H., Kwan, A., Schlaubitz, S., Barsh, G.S., Enns, G.M., and Hudgins, L. (2006). Genitopatellar syndrome: Expanding the phenotype and excluding mutations in LMX1B and TBX4. Am. J. Med. Genet. A. *140*, 1567–1572.
2. Armstrong, L., and Clarke, J.T.R. (2002). Report of a new case of "genitopatellar" syndrome which challenges the importance of absent patellae as a defining feature. J. Med. Genet. *39*, 933–934.
3. Bergmann, C., Spranger, S., Javaher, P., and Ptok, M. (2011). Genitopatellar syndrome, sensorineural hearing loss, and cleft palate. Oral Maxillofac Surg *15*, 103–106.

4. Brugha, R., Kinali, M., Aminu, K., Bridges, N., and Holder, S.E. (2011). Genitopatellar syndrome: A further case. Clin. Dysmorphol. *20*, 163–165.
5. Cormier-Daire, V., Chauvet, M.L., Lyonnet, S., Briard, M.L., Munnich, A., and Le Merrer, M. (2000). Genitopatellar syndrome: A new condition comprising absent patellae, scrotal hypoplasia, renal anomalies, facial dysmorphism, and mental retardation. J. Med. Genet. *37*, 520–524.
6. Goldblatt, J., Wallis, C., and Zieff, S. (1988). A syndrome of hypoplastic patellae, mental retardation, skeletal and genitourinary anomalies with normal chromosomes. Dysmorphol. Clin. Genet. *2*, 91–93.
7. Lammer, E.J., and Abrams, L. (2002). Genitopatellar syndrome: Delineating the anomalies of female genitalia. Am. J. Med. Genet. *111*, 316–318.
8. Lifchez, C.A., Rhead, W.J., Leuthner, S.R., and Lubinsky, M.S. (2003). Genitopatellar syndrome: Expanding the phenotype. Am. J. Med. Genet. A. *122A*, 80–83.
9. Penttinen, M., Koillinen, H., Niinikoski, H., Mäkitie, O., and Hietala, M. (2009). Genitopatellar syndrome in an adolescent female with severe osteoporosis and endocrine abnormalities. Am. J. Med. Genet. A. *149A*, 451–455.
10. Reardon, W. (2002). Genitopatellar syndrome: A recognizable phenotype. Am. J. Med. Genet. *111*, 313–315.
11. Schlaubitz, S., Yatsenko, S.A., Smith, L.D., Keller, K.L., Vissers, L.E., Scott, D.A., Cai, W.W., Reardon, W., Abdul-Rahman, O.A., Lammer, E.J., et al. (2007). Ovotestes and XY sex reversal in a female with an interstitial 9q33.3-q34.1 deletion encompassing NR5A1 and LMX1B causing features of Genitopatellar syndrome. Am. J. Med. Genet. A. *143A*, 1071–1081.
12. Das, D.K. (2009). Psammoma body: A product of dystrophic calcification or of a biologically active process that aims at limiting the growth and spread of tumor? Diagn. Cytopathol. *37*, 534–541.
13. Li, H., and Durbin, R. (2009). Fast and accurate short read alignment with Burrows-Wheeler transform. Bioinformatics *25*, 1754–1760.
14. Li, H., Handsaker, B., Wysoker, A., Fennell, T., Ruan, J., Homer, N., Marth, G., Abecasis, G., and Durbin, R.; 1000 Genome Project Data Processing Subgroup. (2009). The Sequence Alignment/Map format and SAMtools. Bioinformatics *25*, 2078–2079.
15. Wang, K., Li, M., and Hakonarson, H. (2010). ANNOVAR: Functional annotation of genetic variants from high-throughput sequencing data. Nucleic Acids Res. *38*, e164.
16. Liu, X., Jian, X., and Boerwinkle, E. (2011). dbNSFP: A lightweight database of human nonsynonymous SNPs and their functional predictions. Hum. Mutat. *32*, 894–899.
17. UniProt Consortium. (2010). The Universal Protein Resource (UniProt) in 2010. Nucleic Acids Res. *38* (Database issue), D142–D148.
18. Ng, P.C., and Henikoff, S. (2003). SIFT: Predicting amino acid changes that affect protein function. Nucleic Acids Res. *31*, 3812–3814.
19. Marth, G.T., Yu, F., Indap, A.R., Garimella, K., Gravel, S., Leong, W.F., Tyler-Smith, C., Bainbridge, M., Blackwell, T., Zheng-Bradley, X., et al; the 1000 Genomes Project. (2011). The functional spectrum of low-frequency coding variation. Genome Biol. *12*, R84.
20. Thomas, T., Voss, A.K., Chowdhury, K., and Gruss, P. (2000). Querkopf, a MYST family histone acetyltransferase, is required for normal cerebral cortex development. Development *127*, 2537–2548.
21. Champagne, N., Bertos, N.R., Pelletier, N., Wang, A.H., Vezmar, M., Yang, Y., Heng, H.H., and Yang, X.J. (1999). Identification of a human histone acetyltransferase related to monocytic leukemia zinc finger protein. J. Biol. Chem. *274*, 28528–28536.
22. Yang, X.J., and Ullah, M. (2007). MOZ and MORF, two large MYSTic HATs in normal and cancer stem cells. Oncogene *26*, 5408–5419.
23. Doyon, Y., Cayrou, C., Ullah, M., Landry, A.-J., Côté, V., Selleck, W., Lane, W.S., Tan, S., Yang, X.-J., and Côté, J. (2006). ING tumor suppressor proteins are critical regulators of chromatin acetylation required for genome expression and perpetuation. Mol. Cell *21*, 51–64.
24. Ullah, M., Pelletier, N., Xiao, L., Zhao, S.P., Wang, K., Degerny, C., Tahmasebi, S., Cayrou, C., Doyon, Y., Goh, S.-L., et al. (2008). Molecular architecture of quartet MOZ/MORF histone acetyltransferase complexes. Mol. Cell. Biol. *28*, 6828–6843.
25. Surapureddi, S., Yu, S., Bu, H., Hashimoto, T., Yeldandi, A.V., Kashireddy, P., Cherkaoui-Malki, M., Qi, C., Zhu, Y.-J., Rao, M.S., and Reddy, J.K. (2002). Identification of a transcriptionally active peroxisome proliferator-activated receptor alpha -interacting cofactor complex in rat liver and characterization of PRIC285 as a coactivator. Proc. Natl. Acad. Sci. USA *99*, 11836–11841.
26. Lim, J., Hao, T., Shaw, C., Patel, A.J., Szabó, G., Rual, J.-F., Fisk, C.J., Li, N., Smolyar, A., Hill, D.E., et al. (2006). A protein-protein interaction network for human inherited ataxias and disorders of Purkinje cell degeneration. Cell *125*, 801–814.
27. Voss, A.K., and Thomas, T. (2009). MYST family histone acetyltransferases take center stage in stem cells and development. Bioessays *31*, 1050–1061.
28. Kraft, M., Cirstea, I.C., Voss, A.K., Thomas, T., Goehring, I., Sheikh, B.N., Gordon, L., Scott, H., Smyth, G.K., Ahmadian, M.R., et al. (2011). Disruption of the histone acetyltransferase MYST4 leads to a Noonan syndrome-like phenotype and hyperactivated MAPK signaling in humans and mice. J. Clin. Invest. *121*, 3479–3491.
29. Petrij, F., Giles, R.H., Dauwerse, H.G., Saris, J.J., Hennekam, R.C., Masuno, M., Tommerup, N., van Ommen, G.J., Goodman, R.H., Peters, D.J., et al. (1995). Rubinstein-Taybi syndrome caused by mutations in the transcriptional co-activator CBP. Nature *376*, 348–351.
30. Oike, Y., Hata, A., Mamiya, T., Kaname, T., Noda, Y., Suzuki, M., Yasue, H., Nabeshima, T., Araki, K., and Yamamura, K. (1999). Truncated CBP protein leads to classical Rubinstein-Taybi syndrome phenotypes in mice: Implications for a dominant-negative mechanism. Hum. Mol. Genet. *8*, 387–396.
31. Clayton-Smith, J., O'Sullivan, J., Daly, S., Bhaskar, S., Day, R., Anderson, B., Voss, A.K., Thomas, T., Biesecker, L.G., Smith, P., et al. (2011). Whole-exome-sequencing identifies mutations in histone acetyltransferase gene KAT6B in individuals with the Say-Barber-Biesecker variant of Ohdo syndrome. Am. J. Hum. Genet. *89*, 675–681.
32. Day, R., Beckett, B., Donnai, D., Fryer, A., Heidenblad, M., Howard, P., Kerr, B., Mansour, S., Maye, U., McKee, S., et al. (2008). A clinical and genetic study of the Say/Barber/Biesecker/Young-Simpson type of Ohdo syndrome. Clin. Genet. *74*, 434–444.